The Journal of Immunology

# Multiplex B Cell Characterization in Blood, Lymph Nodes, and Tumors from Patients with Malignancies

A. Ali Zirakzadeh, Per Marits, Amir Sherif and Ola Winqvist

*J Immunol* 2013; 190:5847-5855; Prepublished online 29 April 2013;
doi: 10.4049/jimmunol.1203279
http://www.jimmunol.org/content/190/11/5847



*The Journal of Immunology* is published twice each month by
The American Association of Immunologists, Inc.,
9650 Rockville Pike, Bethesda, MD 20814-3994.

Print ISSN: 0022-1767 Online ISSN: 1550-6606.

# Multiplex B Cell Characterization in Blood, Lymph Nodes, and Tumors from Patients with Malignancies

**A. Ali Zirakzadeh,* Per Marits,* Amir Sherif,† and Ola Winqvist***

**B lymphocytes contribute to immune surveillance, by tumor-specific Abs and Ag presentation to T lymphocytes, but are insufficiently studied in humans. In this article, we report a flow cytometric investigation of B lymphocyte subpopulations in blood, lymph nodes (LNs), and malignant tissues from 20 patients operated on because of advanced solid tumors. The CD19$^+$ compartment in peripheral blood was essentially unaltered in patients, as compared with healthy control subjects. In metastatic LNs, signs of B lymphocyte activation were observed, as evidenced by increased proportions of plasmablasts and CD86-expressing cells. In tumor-infiltrating B lymphocytes (TIL-B), both switched memory cells and plasmablasts were expanded, as compared with nonmalignant epithelium. Moreover, pronounced skewing of Igλ/Igκ ratio was evident among TIL-Bs. By spectratype analysis on IgH, we confirmed a monoclonal expansion of the Vh7 family in TIL-B, also present in a tumor-associated LN. Sequencing the clonally expanded Vh7 revealed signs of somatic hypermutation. In conclusion, B lymphocytes in cancer patients exhibit signs of activation in tumor-associated tissues, likely induced by recognition of tumor Ags. Increased numbers of switched memory cells and plasmablasts in combination with clonal expansion and signs of somatic hypermutation suggest a CD4$^+$ T lymphocyte–dependent antitumoral response, which may be exploited for immunotherapy.** ***The Journal of Immunology*****, 2013, 190: 5847–5855.**

Despite modern treatments, cancer remains one of the leading causes of death worldwide. Progress in the field of tumor immunology has made immunotherapy an attractive approach in trying to treat cancer. However, these efforts have mainly focused on tumor-reactive T cells (1–4). Less attention has been paid to B cells and their role in host defense against tumors (5). B cells may contribute to this process in multiple ways, for instance, by presenting Ags to T cells (5, 6). In particular, the high-affinity binding of the BCR to its specific target makes the B cell able to sense and react to small amounts of Ag in the environment, which clearly is an advantage over other APCs. Another way by which B cells can promote a tumor immune response is by producing Abs against tumor Ags, such as Her-2/neu (7). Furthermore, human B cells secrete granzyme B when stimulated with IL-21 (8), which has direct cytotoxic effect against tumor cells. They can also regulate other immune cells by secreting different cytokines and chemokines. Importantly, they can facilitate the formation of CD4$^+$ memory T cells (9) and promote survival and proliferation of activated CD8$^+$ T cells through CD27–CD70 interactions (10).

*Department of Medicine, Unit of Translational Immunology, Karolinska Institutet, 171 76 Stockholm, Sweden; and †Department of Surgical and Perioperative Sciences, Urology and Andrology, Umeå University Hospital, 901 85 Umeå, Sweden

Received for publication November 29, 2012. Accepted for publication March 20, 2013.

This work was supported by the Swedish Cancer Foundation, the Wallenberg Foundation, the Swedish Medical Research Council, and the Karolinska Research Network Program in Immune Modulatory Therapies for Autoimmunity and Cancer.

Address correspondence and reprint requests to Prof. Ola Winqvist, Department of Medicine, Unit of Translational Immunology, Karolinska Institutet, 171 76 Stockholm, Sweden. E-mail address: ola.winqvist@karolinska.se

The online version of this article contains supplemental material.

Abbreviations used in this article: FR3, frame 3; LN, lymph node; MLN, metastatic lymph node; NMLN, nonmetastatic lymph node; NTIL-B, nonmalignant tissue–infiltrating B lymphocyte; TDLN, tumor-draining lymph node; TIL, tumor-infiltrating lymphocyte; TIL-B, tumor-infiltrating B lymphocyte; UBC, urinary bladder cancer.



www.jimmunol.org/cgi/doi/10.4049/jimmunol.1203279

Lymphocytic infiltrates within solid tumors are well-recognized positive predictors of survival (11). Notably, B cells are a significant component of these infiltrates. For example, they have been reported to be present in ~25% of breast cancers and constituted up to 40% of the tumor-infiltrating lymphocyte (TIL) population (12–14). Furthermore, tumor-infiltrating B lymphocytes (TIL-Bs) have been correlated with survival in ovarian cancer. The survival was higher when tumors contained both CD20$^+$ and CD8$^+$ cells than either of the TILs alone, which suggests an immunological cooperation between the two cell populations (15).

B cells in lymph nodes (LNs) may also have a major impact on tumor immune responses. In a murine mouse model, 30–35% of freshly harvested tumor-draining LN (TDLN) cells consisted of CD19$^+$ B cells. CD40 targeting of the TDLN B cells and dendritic cells, in combination with CD3 targeting of T cells, induced a strong antitumor response. However, depleting either B cells or DCs significantly diminished the antitumor response (16). This study illustrates the potential of TDLN B cells to be effective as APCs with generation of more potent effector cells for adoptive immunotherapy. Moreover, in vitro activated TDLN B cells produce a strong humoral tumor response (17).

However, most studies of B cells in cancer have been performed in mouse models. Comparatively little is known about human tumor-associated B cells and their role in cancer biology. It is therefore of great interest to characterize different subpopulations of B cells in cancer patients. For this purpose, we emulated the Freiburg classification of B cells, categorizing them into six distinct subpopulations, including transitional, naive, marginal zone–like, switched memory, CD21$^{low}$ B cells, and class-switched plasmablasts (18–20). By comparing B cell subpopulations from blood, metastatic lymph node, and tumor from patients with malignancies using the Freiburg panel, L chain discrimination, and also BCR cloning, we present evidence for clonal expansion of tumor recognizing B cell clones.

## Materials and Methods

### *Subjects*

Twenty patients were included in the study: 5 with colon cancer; 9 with urinary bladder cancer (UBC); 4 with malignant melanoma, 1 with pancreatic

cancer, and 1 with prostate cancer. Specimens from LNs, the primary tumor, and in some cases, macroscopically normal urinary bladder mucosa were obtained (Table I), immediately put in RPMI 1640 medium (Sigma), and put on ice, awaiting subsequent preparation (see Cell Preparation section). In addition, peripheral blood was collected from the patients and from 14 healthy donors. The remaining part of LNs and primary tumor were subjected to routine histopathological examination. The study was approved by the local ethical committee, and informed consent was given by the patients.

### *Identification of the metastatic LNs*

Identification of metastatic LNs (MLNs) was done by pathological examination or, alternatively, by intracellular flow cytometry against epithelial cell markers, as previously described (21).

### *Cell preparation*

All the obtained specimens were taken care of within 2 h and treated as follows: PBMCs were separated from peripheral blood using density centrifugation (Ficoll-Paque plus; GE Healthcare). Single-cell suspensions from LNs around the tumors, primary tumors, and nonmalignant tissues were isolated by gentle pressure using a glass homogenizer. Primary tumors and urinary bladder specimens were homogenized using GentleMACS Dissociator (Miltenyi Biotec) in 10 ml RPMI 1640 medium (Sigma), containing 1% collagenase/Hyaluronidase solution (StemCell Technologies).

### *Flow cytometry analysis*

After cell preparation, the cells were freshly used for flow cytometry. They were washed with FACS buffer containing PBS, 2.5% bovine growth serum, and 0.05% $NaN_3$, followed by staining with fluorophore-conjugated Abs against B cell surface markers. The following Abs were used: CD19 allophycocyanin-Cy7, IgD FITC, IgM PE-Cy5, CD38 PE-Cy7, Igκ allophycocyanin, Igλ PE, IgG PE-Cy5, CD27 PE, CD21 allophycocyanin, CD40 FITC, CD86 PE-Cy5, CD69 FITC (Becton Dickinson), and IgA FITC (Miltenyi Biotec) The stained cells were investigated using a FACSAria (Becton Dickinson); $2 \times 10^5$ to $1 \times 10^6$ events/sample were collected. The data were analyzed using FACSDiva software. The following Abs were used for identification of MLNs: EpCam AF488 (Fujirebio Diagnostic), mouse anti-human Cytokeratin 20, Cytokeratin 19, Ca19-9 (Dako), and mouse anti-human melanoma (HMB45 + DT101 + BC199; Abcam). The secondary Abs and isotype controls were as follows: mouse IgG2a AF488 (Becton Dickinson), goat anti-mouse IgG allophycocyanin (Jackson), negative control mouse IgG2a, and negative control mouse IgG1 (Dako).

### *Spectratype analysis*

*DNA extraction.* DNA from PBMC, LNs, tumor, and nonmalignant tissue of a UBC patient (61-y-old woman) was extracted using DNA lysis buffer, pH 8.0 (10 mM Tris, 1 mM EDTA, 1% SDS) and proteinase K before incubation in 56°C for 10 min. The DNA was then purified, using phenol:chloroform:isoamyl alcohol 25:24:1 saturated with 10 mM Tris, pH 8.0, 1 mM EDTA (Sigma-Aldrich). After centrifugation, sodium acetate (NaOAC) 3 M and 100% ethanol were added to the upper phase of the samples, stepwise rehydration, and resuspension in ultrapure water.

*PCR.* The 46–52 functional Vh gene segments were grouped into 7 Vh subgroups based on their homology, as previously described (22). Seven forward primers against the frame 3 (FR3) region of each of the seven subgroups were used in conjunction with a universal, 6-FAM–conjugated reverse primer against Jh region (22). The PCR was performed with GoTaq master mix (Promega), according to the manufacturer's recommendations.

*Spectratyping.* For spectratype analysis, Gene Scan 400 HD size standard, Hi-Di Formamide, and ABI 3730 DNA Analyzer (Applied Biosystems) was used as described previously (23). The samples were prepared according to the manufacturer's protocol (Applied Biosystems). The software, Peak Scanner (Applied Biosystems), was used to analyze the data.

### *Sequencing*

The PCR product from the earlier spectratype analysis was purified with QIAquick PCR purification kit (Qiagen). The purified PCR product was then cloned using TOPO TA Cloning Kit for Sequencing with TOP10 chemically competent cells (Invitrogen) and purified using Plasmid Mini Kit (Qiagen). The purified plasmids were sequenced using ABI 3730 DNA analyzer (Applied Biosystems).

### *Statistical analysis*

The flow cytometry data and comparisons between the specimens were analyzed using Student two-tailed unpaired *t* test and Mann–Whitney *U* test in GraphPad Prism software. The comparisons of Igλ/Igκ L chain distributions were analyzed using Fisher's F-test.

## Results

To characterize the tumor-associated B cell compartment in humans, we studied 20 patients with various solid tumors. Details regarding the diagnoses, clinical data, and surgical samples obtained for investigation are shown in Table I.

### *Signs of clonal expansion of circulating B cells from patients with malignant disease*

To investigate B cell subpopulations in peripheral blood from patients with malignant disease, we used the validated Freiburg panel, initially introduced for common variable immunodeficiency diagnosis, using cell-surface markers to categorize $CD19^+$ B cells into six subpopulations (18–20). By flow cytometry, the following $CD19^+$ B cell subpopulations are distinguished in peripheral blood: naive B cells ($IgD^+CD27^-$), marginal zone–like/natural effector B cells ($IgD^+CD27^+$), class-switched memory B cells ($IgD^-CD27^+$), the rare $CD21^{low}$ $CD38^{low}$ B cell population, and transitional B cells ($IgM^{2+}CD38^{2+}$) and plasmablasts ($IgM^-CD38^{3+}$). An example from a healthy blood donor is demonstrated in Fig. 1.

The B cell surface phenotypes of PBMCs from the cancer patients were first compared with that of PBMCs from 10 healthy blood donors (Fig. 2). None of the patients exhibited lymphopenia or abnormal total numbers of B cells in peripheral blood (Supplemental Table I) (15), and there was no significant difference in the proportion of $CD19^+$ lymphocytes, as compared with healthy donors (Fig. 2A, *top left panel*); nor was there any discernible difference in the distribution of B cell subpopulations in patient blood according to the Freiburg panel, with the exception of plasmablasts. The proportion of plasmablasts was significantly lower ($p < 0.05$) in the blood from patients with malignant disease (Fig. 2A, *bottom panel*). Skewing of Igλ/Igκ L chain usage may indicate clonal expansion of B lymphocytes. The Igλ/Igκ L chain ratio on peripheral blood B lymphocytes from healthy donors revealed the expected Igκ dominance, with an Igλ/Igκ L

Table I. Information about the patients, severeness of their disease, and number of samples

| Cancer Types | Patients | Age, y | Sex, M:F | MLN:Patients[a] | NMLN:Patients[a] | Blood[b] | Tumor[b] | Nonmalignant Tissue[b] | Chemotherapy |
|---|---|---|---|---|---|---|---|---|---|
| CC | 5 | 47–69 | 4:1 | 9:5 | — | — | — | — | N |
| UBC | 9 | 53–86 | 7:2 | 4:2 | 17:4 | 8 | 7 | 4 | 2 Y, 7 N |
| MM | 4 | 50–76 | 3:1 | 5:3 | 3:3 | — | — | — | N |
| PC | 1 | 72 | 1:0 | 1:1 | — | — | — | — | N |
| PrC | 1 | 81 | 1:0 | - | 2:1 | 1 | 1 | 1 | N |
| Total | 20 | 47–86 | 16:4 | 19:11 | 22:8 | 9 | 8 | 5 | 2 Y, 11 N |

[a]Number of metastasized and nonmetastasized LNs versus number of patients from whom they were acquired.
[b]Each sample is taken from one patient.
CC, Colon cancer; MM, malignant melanoma; N, no previous neoadjuvant chemotherapy; PC, pancreatic cancer; PrC, prostate cancer; Y, with previous neoadjuvant chemotherapy.

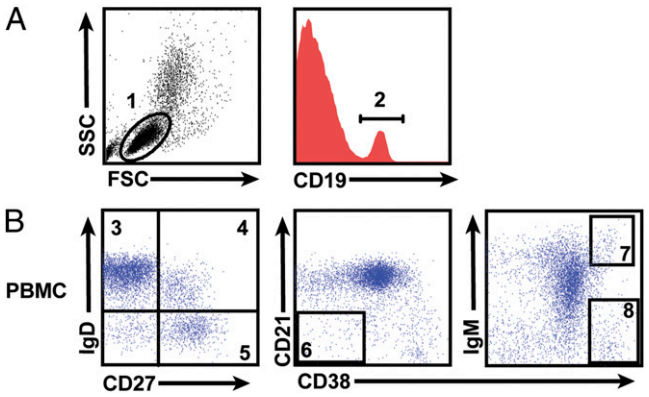


**FIGURE 1.** Multicolor flow cytometry analysis of subpopulations of B cells in blood of cancer patients. A representative example of PBMCs is shown. (**A**) A lymphocyte gate is established on forward (FSC) and side scatter (SSC) characteristics (*left panel*, gate 1), followed by gating on $CD19^+$ cells (*right panel*, gate 2). (**B**) In the Freiburg classification, the following $CD19^+$ B cell subpopulations are defined: $IgD^+$ $CD27^-$ naive (gate 3), $IgD^+$ $CD27^+$ marginal zone–like (gate 4), and $IgD^-$ $CD27^+$ class-switched memory (gate 5). Furthermore, CD21/CD38 and IgM/CD38 dot plots permit distinction of $CD21^{low}$ $CD38^{low}$ (gate 6), $IgM^{2+}$ $CD38^{2+}$ transitional B cells (gate 7), and $IgM^-$ $CD38^{3+}$ plasmablasts (gate 8).

chain ratio of 0.7 (Fig. 2B, *top panel*). However, the Igλ/Igκ L chain ratio among peripheral blood B lymphocytes from patients with malignant disease displayed a significantly increased spreading ($p < 0.05$) compared with the ratios on B lymphocytes from healthy donors, indicating clonal expansions of B lymphocytes in some of the patients (Fig. 2B, *top panel*). However, the proportion of circulating $IgG^+$ B lymphocytes was unaffected (Fig. 2B, *middle panel*). In addition, circulating B lymphocytes from patients with malignant disease did not demonstrate any signs of recent activation because no significant differences with regard to expression of CD69 (Fig. 2B, *bottom panel*), CD86, and CD40 were observed (data not shown).

### *B lymphocytes in MLNs have an activated phenotype*

We decided to investigate B cell subpopulations, isolated from MLNs and nonmetastatic LNs (NMLNs). An example of an LN investigated using the Freiburg panel is shown in Fig. 3A. The distribution of the B lymphocyte populations in the LN appears similar to that observed in peripheral blood, with the exception of an increased proportion of switched memory cells ($IgD^-CD27^+$) and a lower proportion of $IgM^{2+}CD38^{2+}$ transitional B cells (Fig. 3A).

When investigating the B lymphocyte subpopulations in lymph nodes using the Freiburg panel, we first noticed that the fraction of $CD19^+$ B lymphocytes from MLNs was significantly lower than in NMLNs ($p < 0.01$; Fig. 3B), but the balance between naive ($IgD^+$ $CD27^-$) and switched memory cells ($IgD^-CD27^+$) was unaltered. However, the distribution of the other B cell subpopulations was altered in the presence of LN metastasis: in the MLNs, the proportion of marginal zone–like/innate effector B cells ($IgD^+CD27^+$) was significantly decreased ($p < 0.01$; Fig. 3B). In addition, there was a significantly increased proportion of transitional B cells ($IgM^{2+}$ $CD38^{2+}$; $p < 0.05$) and plasmablasts ($IgM^-CD38^+$; $p < 0.001$) in MLNs (Fig. 3B).

Because we found a significant difference in the distribution of Igλ/Igκ L chain usage in peripheral blood (Fig. 2B), we compared

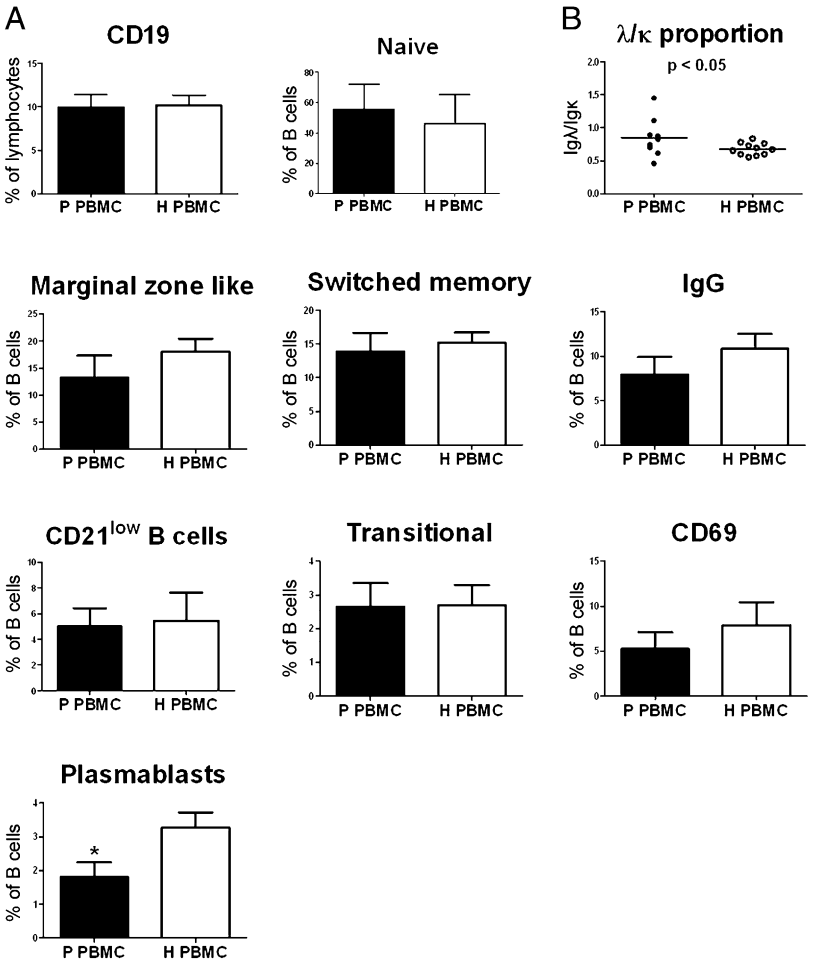


**FIGURE 2.** The $CD19^+$ B cell compartment in peripheral blood from patients and healthy donors. (**A**) Mean percentages of $CD19^+$ B cells in total lymphocytes and of the B cell subpopulations in $CD19^+$ lymphocytes are shown. (**B**, *top panel*) The Igλ/Igκ isotype distribution was determined by flow cytometry. The proportion is calculated by dividing Igλ with Igκ percentages of $CD19^+$ cells. (B, *middle* and *bottom panels*) Percentages of $CD69^+$ and $IgG^+$ cells in $CD19^+$ lymphocytes are shown. Numbers of patients and healthy donors in this experiment are indicated in Table I. The SD of the Igλ/Igκ ratio was calculated using Fisher's F-test. All error bars indicate SEM. Percentages of lymphocyte subpopulations were compared with the Student two-tailed *t* test or Mann–Whitney *U* test. $*p < 0.05$.

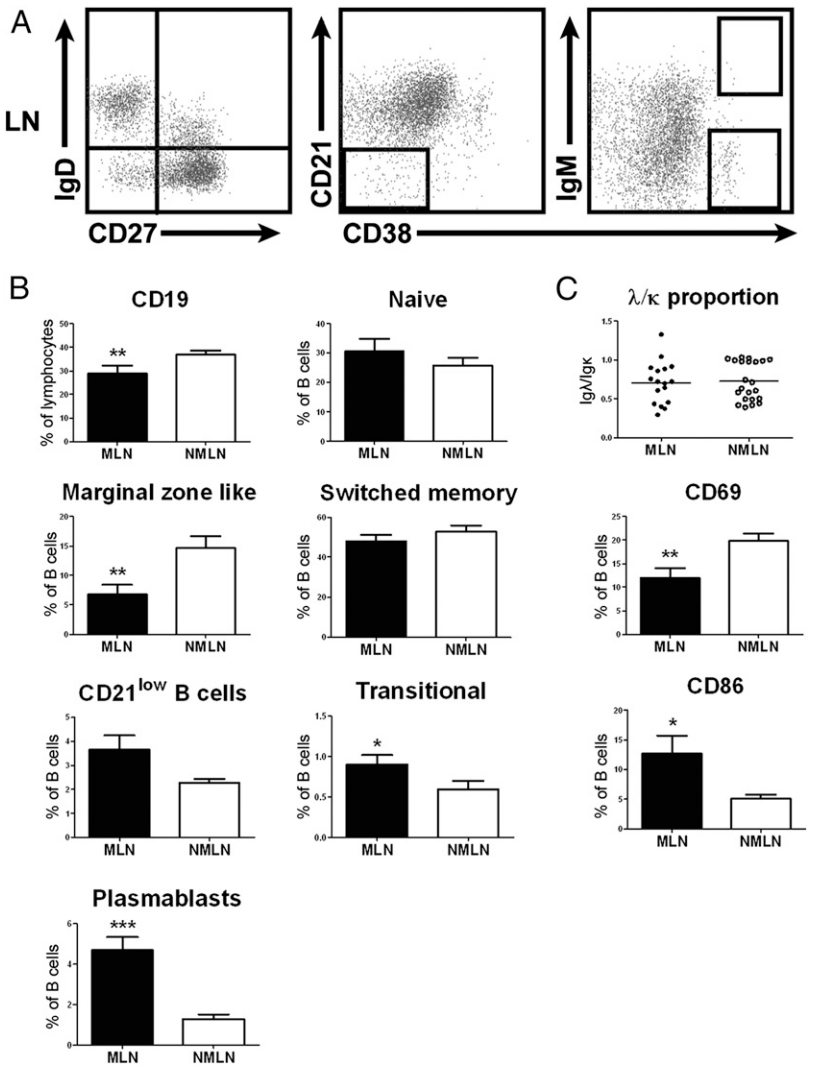


**FIGURE 3.** Comparison between MLNs and NMLNs. (**A**) The Freiburg panel shows subpopulations of $CD19^+$ lymphocytes in a representative example from an LN. (**B**) $CD19^+$ mean percentages of lymphocytes and B cell subpopulations in MLNs and in NMLNs are shown. (**C**, *top panel*) The proportion of Igλ/Igκ light chains was investigated by flow cytometry. The proportion is calculated by dividing Igλ with Igκ percentages of $CD19^+$ cells. (C, *middle* and *bottom panels*) $CD69^+$ and $CD86^+$ B cells are shown. Numbers of MLNs and NMLNs are indicated in Table I. The SD of the Igλ/Igκ ratio was calculated using Fisher's F-test. All error bars indicate SEM. Percentages of lymphocyte subpopulations were compared with the Student two-tailed *t* test or Mann–Whitney *U* test. $*p < 0.05$, $**p < 0.01$, $***p < 0.001$.

the L chain usage in LNs with or without metastases. There was no significant difference in the Igλ/Igκ L chain usage when comparing B cell L chain expression from MLNs and NMLNs (Fig. 3C, *top panel*). However, the distribution of B cell L chain expression in NLMs seem to be bipolar with either a λ or κ dominating usage, whereas the B cell L chain usage in MLNs seems to be distributed in a continuous gradient, suggesting that tumor cells influence L chain usage. To further substantiate the influence of tumor cells on B cell activation, we investigated the expression of the very early activation marker CD69, the costimulatory molecule CD86, and CD40 in LNs with or without metastases. The fraction of $CD69^+$-expressing B cells in MLNs was significantly decreased ($p < 0.01$). However, there was an increased fraction of CD86-expressing B cells in MLNs ($p < 0.05$; Fig. 3C, *lower panel*), whereas there were no significant differences in the $CD40^+$ populations (data not shown).

### *Switched memory B cells and plasmablasts accumulate in tumors*

From eight patients, mainly with UBC, samples from tumor and corresponding nonmalignant tissue were available (Table I), which enabled us to compare TIL-B with the presence of B cell subpopulations in nonmalignant epithelial tissue. Representative plots from these investigations are shown in Fig. 4A and 4B where samples from a UBC patient are shown. There was no difference in the proportion $CD19^+$ B cells retrieved from tumors when compared with B cells from normal tissues. However, the distribution of B cell subpopulations within tumor tissue appeared right-shifted, that is, shifted toward more developed stages of maturation, with significantly increased representation of $IgD^-CD27^+$ switched memory cells ($p < 0.05$) and $IgM^-CD38^+$ plasmablasts ($p < 0.01$). Albeit not reaching significance, there was a corresponding tendency toward decreased representations of naive, marginal zone–like and $CD21^{low}$ B cells in the tumor samples (Fig. 4C). Furthermore, the Igλ/Igκ L chain ratio displayed pronounced skewing among the TIL-Bs ($p < 0.05$) compared with the L chain usage among B cells from normal epithelia (Fig. 4D, *upper panel*). There were no significant differences between $CD69^+$ (Fig. 4D, *lower panel*), $IgG^+$, $CD40^+$, and $CD86^+$ (data not shown) TIL-Bs when compared with B cells from corresponding nonmalignant epithelial tissue.

### *UBC specimens display the same distribution of B cell subtypes*

To investigate whether there was a difference between distributions of B cell subtypes in specimens from a certain cancer type compared with the original data from all patients, we analyzed data from UBC separately. There were no differences between circulating B cell subtypes in UBC compared with healthy control and B cell subtypes in the original data (Fig. 5A). No differences of other markers and distribution of Igλ/Igκ L chain ratio in the two groups of specimens could be seen (Fig. 5B). When comparing B cell subtypes, $CD86^+$, $CD69^+$ B cells, and Igλ/Igκ L chain ratio in MLN with

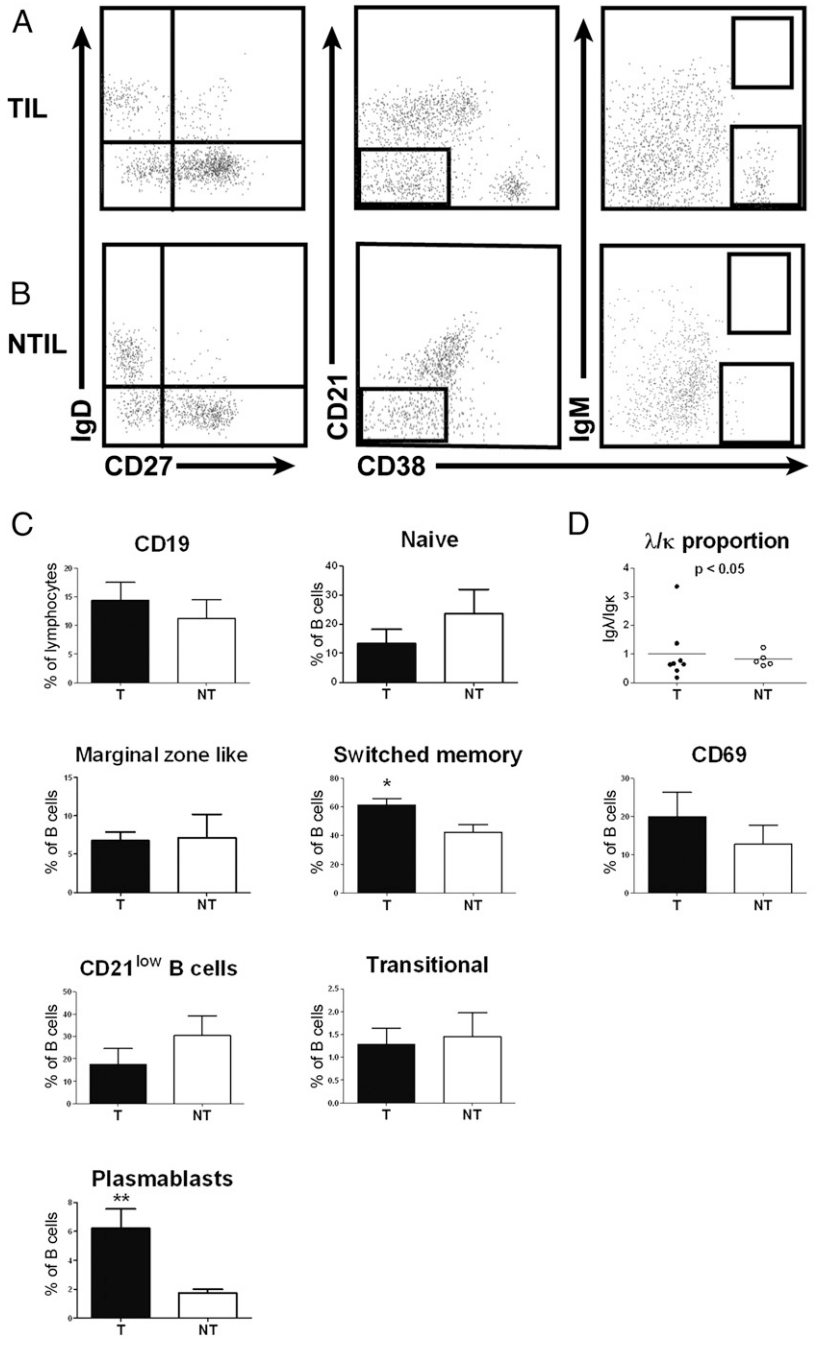


**FIGURE 4.** Comparison between TIL-Bs and NTIL-Bs. (**A**) The Freiburg panel shows subpopulations of $CD19^+$ lymphocytes in a representative example from tumor (**B**) and nonmalignant tissue of a UBC patient. (**C**) The mean percentages of $CD19^+$ lymphocytes and their subpopulations are shown. (**D**, *top panel*) The L chain distribution in tumor tissues was investigated by flow cytometry. The proportion is calculated by dividing Igλ with Igκ percentages of $CD19^+$ cells. (D, *bottom panel*) $CD69^+$ TIL-Bs and NTIL-Bs are shown. Numbers of TIL-Bs and NTIL-Bs are indicated in Table I. The SD of the Igλ/Igκ ratios was calculated using Fisher's F-test. All error bars indicate SEM. Percentages of lymphocyte subpopulations were compared with the Student two-tailed *t* test or Mann–Whitney *U* test. $*p < 0.05$, $**p < 0.01$.

NMLN, no differences could be seen between the two groups of patients (Fig. 6A, 6B). The distributions of B cell subtypes in tumor from UBC patients compared with their counterparts in normal urinary bladder epithelium did not display any differences with data from all patients (Fig. 7A). The same observation could be noticed when $CD69^+$ B cells and Igλ/Igκ ratio in tumors versus nonmalignant tissue were compared in the two groups of patients (Fig. 7B).

### *Corresponding clonal B cell expansion in tumor and adjacent LNs*

The observed skewing of Igλ/Igκ ratios in B cells from blood (Fig. 2B), MLNs (Fig. 3C), and TILs (Fig. 4D) suggested clonal expansion of B cells in response to recognition of tumor Ags. To confirm the presence of clonal expansion, we performed a spectratype analysis investigating the recombination of seven IgH families in B cells from a UBC patient, where B cells from tumor and LN were available for analysis. The spectratype analyses investigating the usage of the heavy chains Vh1–6 did not display any major expansion in any particular CDR3 length, when comparing peaks from tumor, LN, nonmalignant tissue, or PBMCs (Supplemental Figs. 1–3). However, we found one outstanding CDR3 peak when the Vh7 H chain was investigated among B cells from the tumor (Fig. 8). The dominant peak in the LN displayed the same CDR3 length as demonstrated in the overlay plot of tumor and LN (Fig. 8B), thus suggesting the same clonal expansion in the TDLN and among tumor-infiltrating B cells. In a second, more distant LN from the same patient, there was no dominant CDR3 peak. In comparison, B cells from nonmalignant tissue displayed a Gaussian-like distribution in their CDR3 lengths (Fig. 8, *bottom panel*).

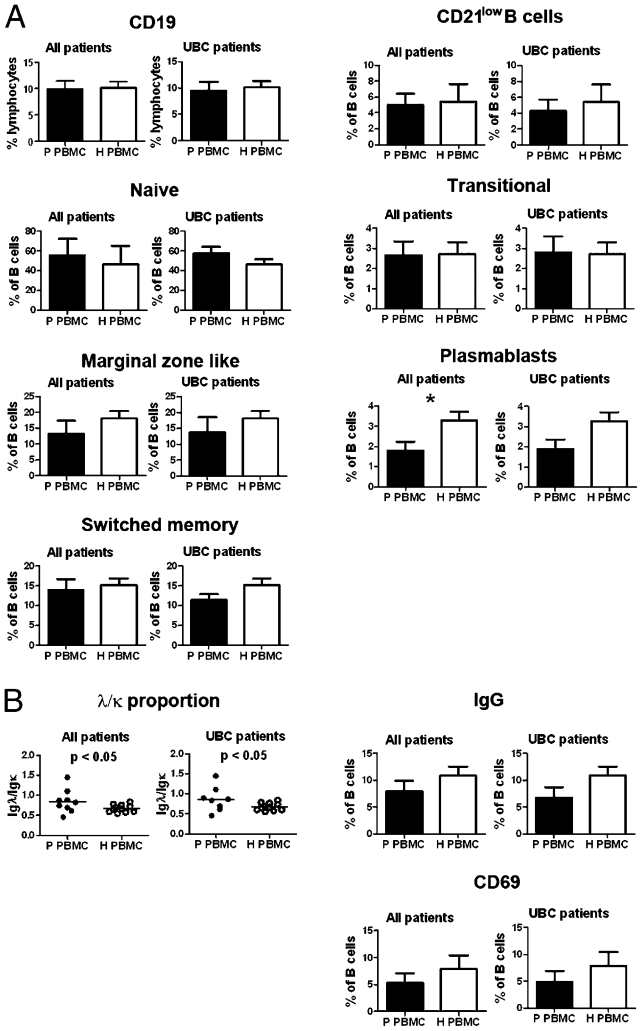


**FIGURE 5.** The CD19$^+$ B cell compartment in peripheral blood from patients and healthy donors in UBC versus all patients. (**A**) Mean percentages of CD19$^+$ B cells in total lymphocytes and of the B cell subpopulations in CD19$^+$ lymphocytes are shown. (**B**) The Igλ/Igκ isotype distribution was determined by flow cytometry. The proportion is calculated by dividing Igλ with Igκ percentages of CD19$^+$ cells. Percentages of CD69$^+$ and IgG$^+$ cells in CD19$^+$ lymphocytes are shown. Numbers of patients and healthy donors in this experiment is indicated in Table I. The SD of the Igλ/Igκ ratio was calculated using Fisher's F-test. All error bars indicate SEM. Percentages of lymphocyte subpopulations was compared with the Student two-tailed *t* test or Mann–Whitney *U* test. $*p < 0.05$.

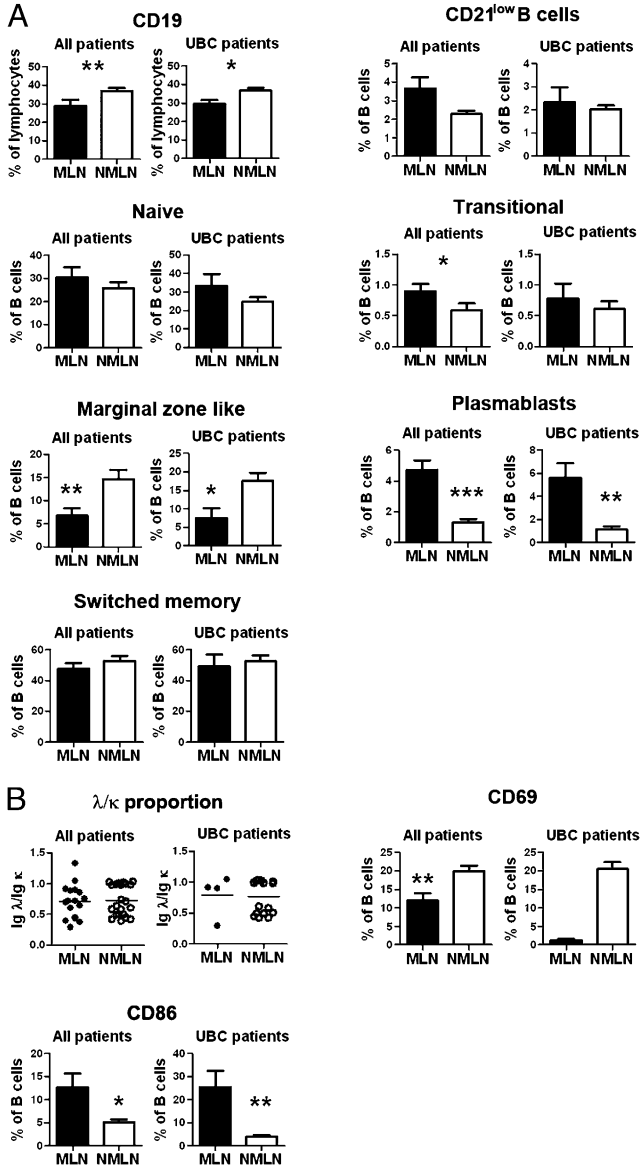


**FIGURE 6.** Comparison between MLNs and NMLNs in UBC versus all patients. (**A**) CD19$^+$ mean percentages of lymphocytes and B cell subpopulations in MLNs and in NMLNs are shown. (**B**) The proportion of Igλ/Igκ light chains was investigated by flow cytometry. The proportion is calculated by dividing Igλ with Igκ percentages of CD19$^+$ cells. CD69$^+$ and CD86$^+$ B cells are shown. Numbers of MLNs and NMLNs are indicated in Table I. The SD of the Igλ/Igκ ratio was calculated using Fisher's F-test. All error bars indicate SEM. Percentages of lymphocyte subpopulations was compared with the Student two-tailed *t* test or Mann–Whitney *U* test. $*p < 0.05$, $**p < 0.01$, $***p < 0.001$.

*Somatic hypermutation of tumor-infiltrating B cells*

To further characterize the clonally expanded H chain in the tumor tissue, we sequenced three clones of the Vh7 family (P1, P3, and P6). Comparing the sequence data from the three clones with published sequences revealed the V-D-J region subfamilies to be IGHV7-04-1*02, IGHD1-07*01, and IGHJ5*02, respectively (Fig. 9A–C). Three bases in FR3 of all the three clones differed compared with the corresponding bases reported from germline sequences (Fig. 9A). One of these mutations was found in a WRCY hotspot motif (Fig. 9A, rectangle) and caused an amino acid change from serine to glycine, whereas the other two were silent mutations. Clone P1 displayed a G-to-A mutation in position 108 of the CDR3, resulting in an amino acid switch from glycine to glutamic acid (Fig. 9D, 9E). The sequencing was carried out twice with forward and reverse primers, and both experiments confirmed the mutations.

## Discussion

During the past few years, increasingly important roles of B cells in the immune system of cancer patients have been reported (12–17, 24). In this study, we describe an increased frequency of plasmablasts in MLNs compared with NMLNs, as well as in tumor versus nonmalignant tissue. Together with the demonstration of a common clonal expansion of tumor-infiltrating B cells in a tumor-associated LN, these observations argue for the presence of tumor-specific B cell responses in cancer patients.

Categorizing subpopulations of B cells has contributed to the understanding of diverse clinical conditions in which B cells play a role, such as common variable immunodeficiency (19) and chronic graft-versus-host disease (25). In this study, we use for the first

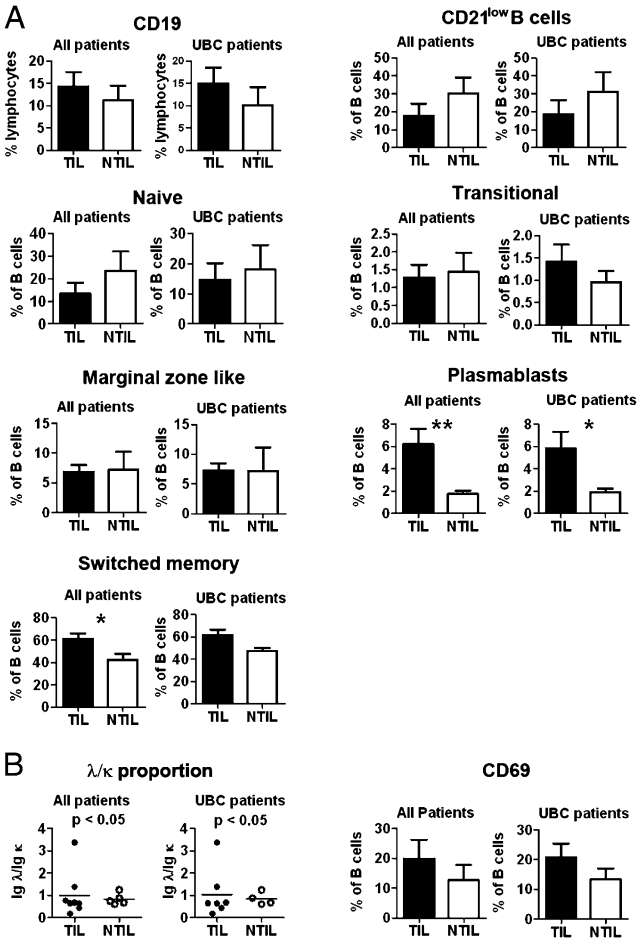


**FIGURE 7.** Comparison between TIL-Bs and NTIL-Bs in UBC versus all patients. (**A**) The mean percentages of $CD19^+$ lymphocytes and their subpopulations are shown. (**B**) The L chain distribution in tumor tissues was investigated by flow cytometry. The proportion is calculated by dividing Igλ with Igκ percentages of $CD19^+$ cells. $CD69^+$ TIL-Bs and NTIL-Bs are shown. Numbers of TIL-Bs and NTIL-Bs are indicated in Table I. The SD of the Igλ/Igκ ratios was calculated using Fisher's F-test. All error bars indicate SEM. Percentages of lymphocyte subpopulations were compared with the Student two-tailed *t* test or Mann–Whitney *U* test. $*p < 0.05$, $**p < 0.01$.

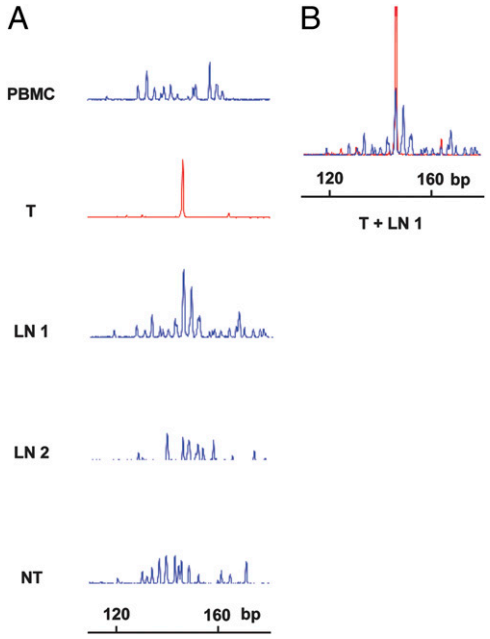


**FIGURE 8.** Spectratype analysis of B cell Vh 7 in PBMC, tumor, LNs, and nonmalignant tissue. (**A**) Spectratype of Vh7 is demonstrated in PBMC, tumor (T), LN 1, LN 2, and nonmalignant tissue (NT) of a UBC patient. The size range of the gene products are given in base pairs. (**B**) Alignment of B cell Vh7 product in tumor (T) and in LN 1. The size range of the DNA products is given in base pairs.

time, to our knowledge, the well-described Freiburg panel to characterize B cell subpopulations from cancer patients. Comparison between $CD19^+$ B cells in healthy blood and in patient blood illustrated no significant difference (Fig. 2A), nor was any difference observed when comparing TIL-Bs and nonmalignant tissue–infiltrating B lymphocytes (NTIL-Bs; Fig. 3A). However, the $CD19^+$ cells occupied a smaller proportion of the lymphocyte compartment in MLNs compared with NMLNs (Fig. 4A). Unfortunately, whether this is due to reduced absolute numbers or is secondary to T cell expansion cannot be deduced from available data. Likewise, the reduced proportion of marginal zone–like B cells in MLNs (Fig. 3A) remains unexplained. As expected, the mean percentage of naive B cells was higher in peripheral blood than in LNs and lower still within the tumor and nonmalignant tissue (Figs. 2–4), whereas the reverse is true for switched memory cells. Interestingly, a higher mean percentage of switched memory B cells in tumors than in normal epithelium was evident, which may indicate tumor Ag encounter and/or recruitment of Ag-specific B cells (Fig. 4A). This interpretation is reinforced by the higher mean percentage of plasmablasts within tumors as compared with their counterparts in nonmalignant tissue (Fig. 4A). It is tempting to speculate that the lower representation of plasmablasts in peripheral blood of cancer patients as compared with healthy blood donors reflects homing of these cells to tumor sites. Comparison of plasmablasts in MLNs and NMLNs also shows a higher mean percentage in the former (Fig. 3A). Likewise, the proportion of CD86-expressing B cells increased in the presence of metastasis, indicating tumor-specific activation of B cells. Notably, the proportion of $CD69^+$ B cells was lower in MLNs compared with NMLNs and there was no significant difference between any of the activation markers in tumor tissues as compared with normal epithelia. This may be explained by the different kinetics displayed by the markers upon Ag-specific activation, where CD69 is rapidly downregulated, whereas CD86 expression is more long-lasting (26, 27). Interestingly, the mean percentage of transitional B cells was higher in MLNs than in NMLNs. Although the absolute cell numbers in this compartment is low, the observation is intriguing. One possible explanation is increased de novo recruitment of precursor B cells, and alternatively that an immunosuppressive milieu is created by the tumor, which hampers their maturation to B cells.

The origin and function of the $CD21^{low}$ B cells in the Freiburg panel has been debated. Their numbers are increased during chronic viral infection, as well as in certain immunodeficiencies and autoimmune diseases (19, 28). Some authors have suggested that they resemble innate-like tissue homing B cells (29), but their exact role is likely dependent on the underlying condition. In the setting of HIV infection, two distinct subpopulations have been described, namely, $CD27^+$-activated mature B cells and $CD27^-$-exhausted tissue-like memory B cells (30). In this study, $CD21^{low}$ B cells were mostly present in tumors and nonmalignant tissues, which is in accordance with the tissue homing properties described by others, and ~50% of the population in both tumors and nonmalignant tissues expressed $CD27^+$ (data not shown). Although their functional status remains to be investigated, their numbers were not significantly different between tumors and normal epithelia; thus, their differentiation does not appear to be

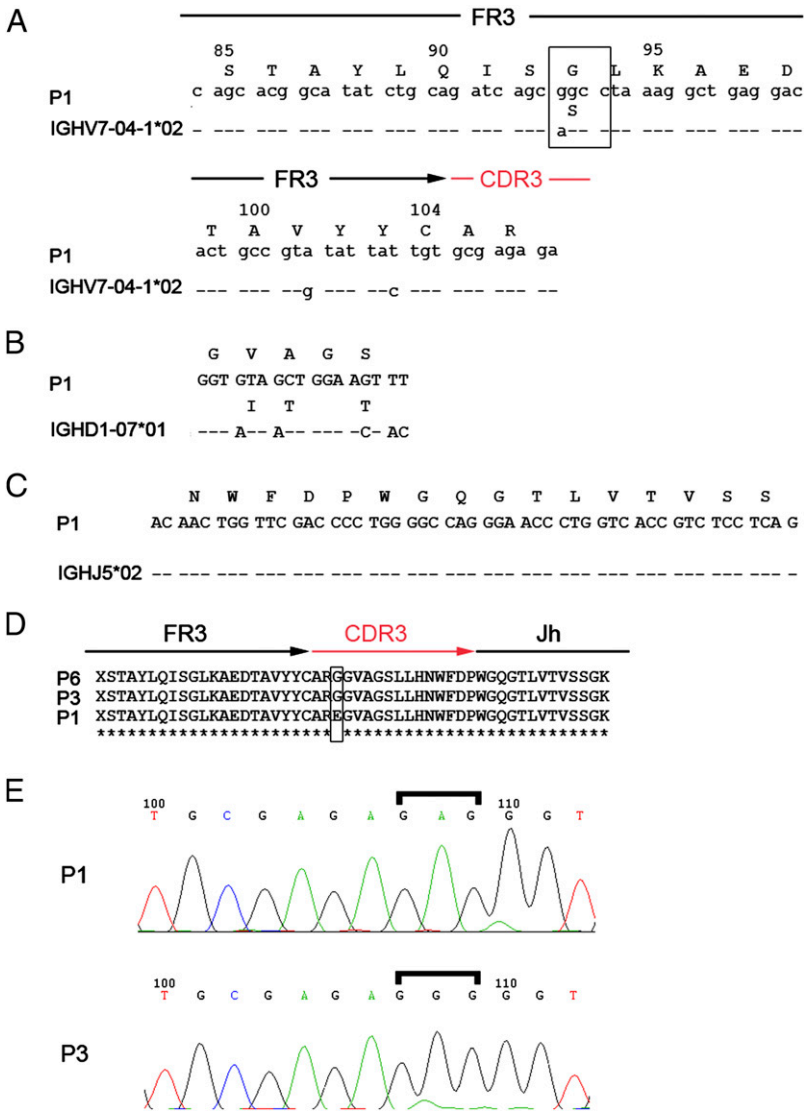


**FIGURE 9.** Vh7 sequence analysis of monoclonal TIL-Bs. (**A**) Alignment between parts of a Vh7 segment of a representative clone (P1) from monoclonal TIL-Bs and the closest suggested germline gene sequence (IGHV7-04-01*2) by Joinsolver. Parts of FR3 and CDR3 are shown. Square highlights WRCY hotspot motif. (**B**) Suggested D-region of a representative clone P1 aligned with its germline counterpart. (**C**) Jh alignment between P1 clone and corresponding germline sequence according to Joinsolver. (**D**) Three Vh7 clones of the same expansion in tumor, P1, P3, and P6, aligned based on amino acid outcome. Square highlights nonhomology of P1. (**E**) Chromatograms of P1 and P3 clones, showing the single base difference causing amino acid change in CDR3 from (D). Brackets highlight codons for the changed amino acids.

influenced by the presence of tumor Ag. On the contrary, the increased numbers of plasmablasts in tumors and MLNs, and the higher percentage of switched memory B cells in MLNs obviously indicate tumor-specific T cell–dependent activation and differentiation of B cells. This process, signified by somatic hypermutation and germinal center formation, also explains the increased skewing and spreading of Igλ/Igκ ratio in patient samples (Figs. 2B, 3B, 4B). Somatic hypermutation is characterized by single base substitutions resulting in a characteristic mutation pattern (31–33). Our sequencing of the Vh7 clone showed a WRCY hotspot motif, which often appears after a mutation in WRC motif caused by activation-induced cytidine deaminase (34, 35). This potential activation-induced cytidine deaminase–dependent mutation strengthens the hypothesis of B cell somatic hypermutation in TIL and in MLNs, and again suggests a T cell–driven response. Certainly, this response may be because of a microbial peptide or stress ligands expressed by the malignant urothelium, but given its context, we consider it more likely to be elicited by tumor Ags. One of our three sequenced clones, P1, contained a single base difference in CDR3 compared with the other clones, which also may represent a somatic hypermutation.

The presence of clonal B cell expansions is formally demonstrated by the spectratype analysis, where we were able to demonstrate a monoclonal expansion of TIL-Bs also present in a tumor-associated LN (Fig. 8). Restricted Ig gene expression in TIL-Bs has been described by others (36, 37). Some investigators have suggested that this expansion occurs within the tumor tissue and in tumor-associated germinal centers (36). By contrast, our result shed light to another option where a tumor-draining LN could be the origin of the B cell response in our study. Merely spectratype analysis is only suggestive. Sequencing of the H chain in the tumor-associated LN is necessary to demonstrate this issue. Notably, we also observed skewing of Igλ/Igκ ratio in some NMLNs (Fig. 3B). This is not surprising; because LNs were in close proximity to the tumor, some, or most of these, are likely tumor draining, and thus may have received soluble tumor debris in vivo, resulting in B cell activation.

In many reports, Ag-experienced TIL-Bs correlate with survival time of patients with different cancer types (38–41). In studies with TIL-Bs in ovarian cancer and breast carcinomas, somatic hypermutation and clonal B cell expansion were shown, using Vh gene analysis. In addition, TIL-Bs displayed class-switching and Ag-presenting phenotypes (40, 41). These observations correlate with our results from TIL-Bs, indicating Ag-dependent tumor response in malignancies.

Taken together, our results suggest that B cell activation patterns reflect a T cell–dependent humoral response to tumors. This underscores the role of B cells as APCs, which is also highlighted

by the higher percentage of $CD86^+$ B cells in MLNs. It has been demonstrated that TDLN B cells in mice can be efficient APCs (16, 17). Yet, it remains to be demonstrated whether they play this role in humans with solid tumors. We have previously described that a tumor-specific Th1 response is present in sentinel LNs in colon and bladder cancer (42, 43), and that sentinel node–acquired $CD4^+$ T cells are promising for use in adoptive immunotherapies (1). In this study, we emulated sentinel node–resident total APCs for ex vivo T cell activation and expansion. Enrichment of tumor-specific B cells as an alternative APC population is a theoretically appealing alternative that deserves to be investigated.

## Disclosures

The authors have no financial conflicts of interest.

## References


1. Karlsson, M., P. Marits, K. Dahl, T. Dagöö, S. Enerbäck, M. Thörn, and O. Winqvist. 2010. Pilot study of sentinel-node-based adoptive immunotherapy in advanced colorectal cancer. *Ann. Surg. Oncol.* 17: 1747–1757.
2. Sherif, A., M. N. Hasan, P. Marits, M. Karlsson, O. Winqvist, and M. Thörn. 2010. Feasibility of T-cell-based adoptive immunotherapy in the first 12 patients with advanced urothelial urinary bladder cancer. Preliminary data on a new immunologic treatment based on the sentinel node concept. *Eur. Urol.* 58: 105–111.
3. Rosenberg, S. A., J. C. Yang, R. M. Sherry, U. S. Kammula, M. S. Hughes, G. Q. Phan, D. E. Citrin, N. P. Restifo, P. F. Robbins, J. R. Wunderlich, et al. 2011. Durable complete responses in heavily pretreated patients with metastatic melanoma using T-cell transfer immunotherapy. *Clin. Cancer Res.* 17: 4550–4557.
4. Rosenberg, S. A., and M. E. Dudley. 2004. Cancer regression in patients with metastatic melanoma after the transfer of autologous antitumor lymphocytes. *Proc. Natl. Acad. Sci. USA* 101(Suppl. 2): 14639–14645.
5. Yanaba, K., J. D. Bouaziz, T. Matsushita, C. M. Magro, E. W. St Clair, and T. F. Tedder. 2008. B-lymphocyte contributions to human autoimmune disease. *Immunol. Rev.* 223: 284–299.
6. Rodríguez-Pinto, D. 2005. B cells as antigen presenting cells. *Cell. Immunol.* 238: 67–75.
7. Reuschenbach, M., M. von Knebel Doeberitz, and N. Wentzensen. 2009. A systematic review of humoral immune responses against tumor antigens. *Cancer Immunol. Immunother.* 58: 1535–1544.
8. Hagn, M., E. Schwesinger, V. Ebel, K. Sontheimer, J. Maier, T. Beyer, T. Syrovets, Y. Laumonnier, D. Fabricius, T. Simmet, and B. Jahrsdörfer. 2009. Human B cells secrete granzyme B when recognizing viral antigens in the context of the acute phase cytokine IL-21. *J. Immunol.* 183: 1838–1845.
9. Whitmire, J. K., M. S. Asano, S. M. Kaech, S. Sarkar, L. G. Hannum, M. J. Shlomchik, and R. Ahmed. 2009. Requirement of B cells for generating CD4+ T cell memory. *J. Immunol.* 182: 1868–1876.
10. Deola, S., M. C. Panelli, D. Maric, S. Selleri, N. I. Dmitrieva, C. Y. Voss, H. Klein, D. Stroncek, E. Wang, and F. M. Marincola. 2008. Helper B cells promote cytotoxic T cell survival and proliferation independently of antigen presentation through CD27/CD70 interactions. *J. Immunol.* 180: 1362–1372.
11. Nelson, B. H. 2010. CD20+ B cells: the other tumor-infiltrating lymphocytes. *J. Immunol.* 185: 4977–4982.
12. Coronella-Wood, J. A., and E. M. Hersh. 2003. Naturally occurring B-cell responses to breast cancer. *Cancer Immunol. Immunother.* 52: 715–738.
13. Chin, Y., J. Janseens, J. Vandepitte, J. Vandenbrande, L. Opdebeek, and J. Raus. 1992. Phenotypic analysis of tumor-infiltrating lymphocytes from human breast cancer. *Anticancer Res.* 12: 1463–1466.
14. Marsigliante, S., L. Biscozzo, A. Marra, G. Nicolardi, G. Leo, G. B. Lobreglio, and C. Storelli. 1999. Computerised counting of tumour infiltrating lymphocytes in 90 breast cancer specimens. *Cancer Lett.* 139: 33–41.
15. Milne, K., M. Köbel, S. E. Kalloger, R. O. Barnes, D. Gao, C. B. Gilks, P. H. Watson, and B. H. Nelson. 2009. Systematic analysis of immune infiltrates in high-grade serous ovarian cancer reveals CD20, FoxP3 and TIA-1 as positive prognostic factors. *PLoS ONE* 4: e6412.
16. Li, Q., A. C. Grover, E. J. Donald, A. Carr, J. Yu, J. Whitfield, M. Nelson, N. Takeshita, and A. E. Chang. 2005. Simultaneous targeting of CD3 on T cells and CD40 on B or dendritic cells augments the antitumor reactivity of tumor-primed lymph node cells. *J. Immunol.* 175: 1424–1432.
17. Li, Q., S. Teitz-Tennenbaum, E. J. Donald, M. Li, and A. E. Chang. 2009. In vivo sensitized and in vitro activated B cells mediate tumor regression in cancer adoptive immunotherapy. *J. Immunol.* 183: 3195–3203.
18. Wehr, C., T. Kivioja, C. Schmitt, B. Ferry, T. Witte, E. Eren, M. Vlkova, M. Hernandez, D. Detkova, P. R. Bos, et al. 2008. The EUROclass trial: defining subgroups in common variable immunodeficiency. *Blood* 111: 77–85.
19. Warnatz, K., and M. Schlesier. 2008. Flowcytometric phenotyping of common variable immunodeficiency. *Cytometry B Clin. Cytom.* 74: 261–271.
20. Eibel, H., U. Salzer, and K. Warnatz. 2010. Common variable immunodeficiency at the end of a prospering decade: towards novel gene defects and beyond. *Curr. Opin. Allergy Clin. Immunol.* 10: 526–533.
21. Karlsson, M., O. Nilsson, M. Thörn, and O. Winqvist. 2008. Detection of metastatic colon cancer cells in sentinel nodes by flow cytometry. *J. Immunol. Methods* 334: 122–133.
22. van Dongen, J. J., A. W. Langerak, M. Brüggemann, P. A. Evans, M. Hummel, F. L. Lavender, E. Delabesse, F. Davi, E. Schuuring, R. García-Sanz, et al. 2003. Design and standardization of PCR primers and protocols for detection of clonal immunoglobulin and T-cell receptor gene recombinations in suspect lymphoproliferations: report of the BIOMED-2 Concerted Action BMH4-CT98-3936. *Leukemia* 17: 2257–2317.
23. Hässler, S., C. Ramsey, M. C. Karlsson, D. Larsson, B. Herrmann, B. Rozell, M. Backheden, L. Peltonen, O. Kämpe, and O. Winqvist. 2006. Aire-deficient mice develop hematopoetic irregularities and marginal zone B-cell lymphoma. *Blood* 108: 1941–1948.
24. Al-Shibli, K. I., T. Donnem, S. Al-Saad, M. Persson, R. M. Bremnes, and L. T. Busund. 2008. Prognostic effect of epithelial and stromal lymphocyte infiltration in non-small cell lung cancer. *Clin. Cancer Res.* 14: 5220–5227.
25. Kuzmina, Z., H. T. Greinix, R. Weigl, U. Körmöczi, A. Rottal, S. Frantal, S. Eder, and W. F. Pickl. 2011. Significant differences in B-cell subpopulations characterize patients with chronic graft-versus-host disease-associated dysgammaglobulinemia. *Blood* 117: 2265–2274.
26. López-Cabrera, M., A. G. Santis, E. Fernández-Ruiz, R. Blacher, F. Esch, P. Sánchez-Mateos, and F. Sánchez-Madrid. 1993. Molecular cloning, expression, and chromosomal localization of the human earliest lymphocyte activation antigen AIM/CD69, a new member of the C-type animal lectin superfamily of signal-transmitting receptors. *J. Exp. Med.* 178: 537–547.
27. Hathcock, K. S., G. Laszlo, C. Pucillo, P. Linsley, and R. J. Hodes. 1994. Comparative analysis of B7-1 and B7-2 costimulatory ligands: expression and function. *J. Exp. Med.* 180: 631–640.
28. Moir, S., and A. S. Fauci. 2009. B cells in HIV infection and disease. *Nat. Rev. Immunol.* 9: 235–245.
29. Rakhmanov, M., B. Keller, S. Gutenberger, C. Foerster, M. Hoenig, G. Driessen, M. van der Burg, J. J. van Dongen, E. Wiech, M. Visentini, et al. 2009. Circulating CD21low B cells in common variable immunodeficiency resemble tissue homing, innate-like B cells. *Proc. Natl. Acad. Sci. USA* 106: 13451–13456.
30. Moir, S., J. Ho, A. Malaspina, W. Wang, A. C. DiPoto, M. A. O'Shea, G. Roby, S. Kottilil, J. Arthos, M. A. Proschan, et al. 2008. Evidence for HIV-associated B cell exhaustion in a dysfunctional memory B cell compartment in HIV-infected viremic individuals. *J. Exp. Med.* 205: 1797–1805.
31. Golding, G. B., P. J. Gearhart, and B. W. Glickman. 1987. Patterns of somatic mutations in immunoglobulin variable genes. *Genetics* 115: 169–176.
32. Betz, A. G., C. Rada, R. Pannell, C. Milstein, and M. S. Neuberger. 1993. Passenger transgenes reveal intrinsic specificity of the antibody hypermutation mechanism: clustering, polarity, and specific hot spots. *Proc. Natl. Acad. Sci. USA* 90: 2385–2388.
33. Phung, Q. H., D. B. Winter, A. Cranston, R. E. Tarone, V. A. Bohr, R. Fishel, and P. J. Gearhart. 1998. Increased hypermutation at G and C nucleotides in immunoglobulin variable genes from mice deficient in the MSH2 mismatch repair protein. *J. Exp. Med.* 187: 1745–1751.
34. Larijani, M., D. Frieder, W. Basit, and A. Martin. 2005. The mutation spectrum of purified AID is similar to the mutability index in Ramos cells and in ung($^{-/-}$) msh2($^{-/-}$) mice. *Immunogenetics* 56: 840–845.
35. Pham, P., R. Bransteitter, J. Petruska, and M. F. Goodman. 2003. Processive AID-catalysed cytosine deamination on single-stranded DNA simulates somatic hypermutation. *Nature* 424: 103–107.
36. Coronella, J. A., C. Spier, M. Welch, K. T. Trevor, A. T. Stopeck, H. Villar, and E. M. Hersh. 2002. Antigen-driven oligoclonal expansion of tumor-infiltrating B cells in infiltrating ductal carcinoma of the breast. *J. Immunol.* 169: 1829–1836.
37. O'Brien, P. M., E. Tsirimonaki, D. W. Coomber, D. W. Millan, J. A. Davis, and M. S. Campo. 2001. Immunoglobulin genes expressed by B-lymphocytes infiltrating cervical carcinomas show evidence of antigen-driven selection. *Cancer Immunol. Immunother.* 50: 523–532.
38. Erdag, G., J. T. Schaefer, M. E. Smolkin, D. H. Deacon, S. M. Shea, L. T. Dengel, J. W. Patterson, and C. L. Slingluff, Jr. 2012. Immunotype and immunohistologic characteristics of tumor-infiltrating immune cells are associated with clinical outcome in metastatic melanoma. *Cancer Res.* 72: 1070–1080.
39. Coronella, J. A., P. Telleman, G. A. Kingsbury, T. D. Truong, S. Hays, and R. P. Junghans. 2001. Evidence for an antigen-driven humoral immune response in medullary ductal breast cancer. *Cancer Res.* 61: 7889–7899.
40. Nielsen, J. S., R. A. Sahota, K. Milne, S. E. Kost, N. J. Nesslinger, P. H. Watson, and B. H. Nelson. 2012. CD20+ tumor-infiltrating lymphocytes have an atypical CD27- memory phenotype and together with CD8+ T cells promote favorable prognosis in ovarian cancer. *Clin. Cancer Res.* 18: 3281–3292.
41. Nzula, S., J. J. Going, and D. I. Stott. 2003. Antigen-driven clonal proliferation, somatic hypermutation, and selection of B lymphocytes infiltrating human ductal breast carcinomas. *Cancer Res.* 63: 3275–3280.
42. Marits, P., M. Karlsson, K. Dahl, P. Larsson, A. Wanders, M. Thörn, and O. Winqvist. 2006. Sentinel node lymphocytes: tumour reactive lymphocytes identified intraoperatively for the use in immunotherapy of colon cancer. *Br. J. Cancer* 94: 1478–1484.
43. Marits, P., M. Karlsson, A. Sherif, U. Garske, M. Thörn, and O. Winqvist. 2006. Detection of immune responses against urinary bladder cancer in sentinel lymph nodes. *Eur. Urol.* 49: 59–70.